RSC Advances

ROYAL SOCIETY OF CHEMISTRY

www.rsc.org/advances

Microwave assisted exfoliation method to develop platinum-decorated graphene nanosheets as a low cost counter electrode for dye-sensitized solar cells

K. Saranya[1], N. Sivasankar [2] and A. Subramania[1]*

1. Electrochemical Energy Research Lab, Centre for Nanoscience and Technology, Pondicherry University, Puducherry - 605 014, India.
2. Department of Metallurgical Engineering & Materials Science, Indian Institute of Technology-Bombay, Mumbai, India-400076

*Corresponding Author E-mail: a.subramania@gmail.com

*Phone: +91413 2654980, Fax: +91413 2655348.

ABSTRACT

Graphene nanosheets (GNs) are prepared from natural graphite by a simple ecofriendly microwave assisted exfoliation technique. The as prepared GNs are decorated with platinum (Pt) nanoparticles by a simple chemical reduction method and used as a low cost counter electrode (CE) material for dye-sensitized solar cells (DSSCs). Structure and morphology of the prepared GNs and Pt decorated GNs (Pt-GNs) are evaluated by X-ray diffraction (XRD), Raman spectroscopy, scanning electron microscopy (SEM), transmission electron microscope (TEM) and selected area electron diffraction (SAED) studies. The electrochemical behavior of GNs and Pt-GNs are compared with std. Pt using cyclic voltammetry (CV) and electrochemical impedance spectroscopy (EIS) studies. These studies indicate that the Pt-GNs based counter electrode offered superior electrocatalytic activity towards I^-/I_3^- redox mediator with enhanced charge transfer rate and exchange current density at the electrode/electrolyte interface over std. Pt and GNs based counter electrodes. DSSCs are fabricated with std. Pt, GNs and Pt-GNs to find out the photovoltaic performance under 1 Sun illumination (100 mW cm^{-2}, AM 1.5). It is found

that the cell fabricated with 1 wt. % Pt decorated GNs as counter electrode showed 11% of improvement in photovoltaic cell efficiency than the cell assembled with std. platinum and other reported graphene-Pt based composites as counter electrodes.

Keywords: Dye-sensitized solar cell, Graphene, Counter electrode, Platinum decorated graphene.

Introduction

Dye-sensitized solar cells have acquired considerable attention as an alternative photovoltaic device for conventional solar cells due to its high performance, low cost, flexibility, light weight, simple fabrication process and several industrial and commercial applications.[1-3] The first DSSC was developed by Gratzel et al. in 1991. Till date, maximum efficiency achieved with DSSC is 13% [4], which can act as significant alternative to conventional silicon based solar cells. In general, DSSC is composed of a wide band gap n-type semiconductor, TiO_2 coated on transparent conducting oxide (TCO) as photoanode which has monolayer of adsorbed dye molecules, an electrolyte with a redox couple (I_3^-/I^-) dissolved in an organic solvent and a counter electrode.[5] When the photo-electrochemical cell is exposed to light, the electron of dye gets excited from highest occupied molecular orbital (HOMO) to lowest unoccupied molecular orbital (LUMO). The electron is then transferred to photoanode and the dye is regenerated by oxidation I^- to I_3^- in the electrolyte. The main task of counter electrode material is to collect the electrons from the external circuit and to regenerate the redox couple of electrolyte. Typically, a counter electrode material requires good electrocatalytic activity, high conductivity and large surface area and it should also speed up the reduction reaction of tri-iodide into iodide ($I_3^- + e^- \rightarrow I^-$).[6] Platinum is exploited as CE material in majority of DSSCs because of its superior

electrocatalytic performance and conductivity. Nevertheless, Pt is expensive, rare metal and its electrocatalytic activity diminishes with prolong operation. This is due to the formation of platinum iodide (PtI_4) by corrosion of Pt in triiodide containing electrolyte.[7] Moreover, platinized CEs require thermal annealing or sputtering which enhances the cost of mass production and hence hinders the commercialization of DSSC. In order to make cell inexpensive, the conventional platinum counter electrode is replaced by relatively more abundant alternate materials. Various transition metal oxides, chalcogenides, carbides, nitrides, phosphides and their composites have been introduced as counter electrode materials.[8] So far, various allotropes of carbonaceous materials such as mesoporous carbon, activated carbon, carbon nanotubes (CNTs), graphite, graphene and conducting polymers and their composites have also been investigated as counter electrode materials for DSSCs. [9-14] Recently, graphene has drawn more attention than other carbonaceous materials owing to its interesting properties such as good electrochemical activity, strong mechanical strength, high electrical, thermal conductivity, electrochemical stability, large surface area etc.

Hsieh et el. reported a standalone graphene as CE for DSSC that exhibited lower efficiency than Pt based counter electrodes. This can be attributed to the lower amount of defective sites due to its highly oriented graphitic structure. This can be eliminated by increasing the number of defect sites or by forming composites. [15,16] Graphene have been composited with metal nanoparticles, conducting polymers and chalcogenides to use as counter electrodes for DSSCs.[17-19] Recently, Kim et al. prepared aqueous dispersible graphene-Pt composite using a one pot chemical reduction method and showed 0.68% improvement in cell efficiency with 10% Pt loading in comparison with pure platinized CE.[19] Cheng et al. prepared graphene-Pt composite by growing graphene by chemical vapor deposition (CVD) followed by sputtering of Pt and

achieved an improvement of 1.78% in photo-conversion efficiency (PCE).[21] Dao et al. synthesized graphene-Pt nanohybrid using modified Hummer method followed by reduction of Pt under Ar plasma and achieved an improvement of 5% in PCE.[22] Tjoa et al. synthesize graphene-Pt composite by photochemical technique and achieved an improvement of 8%.[23] So far, the maximum achieved improvement in photovoltaic cell efficiency for graphene-Pt composites is not more than 8%, when compared to platinum.[24-26] In the above mentioned methods, graphene oxide is synthesised mainly using modified Hummer's method or Staudenmaier method. These methods are time consuming, involve toxic and harsh chemicals which are detrimental to environment and also require higher annealing temperature for exfoliation.[27, 28] Even though, there are very few reports are available for the preparation of exfoliated graphene and metal (Fe, Pt and Pd) decorated graphene by microwave irradiation method and used as electrocatalysts in glucose biosensors.[29-31] But, there is no report on the use of microwave assisted exfoliated graphene nanosheets as counter electrode for DSSCs.

Hence, in the present investigation, graphene nanosheets were prepared using a microwave assisted exfoliation method and then decorated with platinum by a simple chemical reduction method and used as counter electrode for DSSC. This method lowers the cost and time consumption for production. The structure and morphology of Pt-GNs were confirmed by XRD, Raman spectroscopy and SEM. The electrochemical behavior of the prepared Pt decorated GNs was evaluated by cyclic voltammetry and AC-impedance techniques. Photovoltaic performance of DSSC fabricated with 1 wt.% of Pt decorated GNs as counter electrode was compared with the DSSC fabricated with std. Pt and GNs as counter electrodes.

Experimental

Materials used

Natural graphite AR grade (Himedia), Ammonium persulfate (Rankem), Hydrogen peroxide (Merck), Chloroplatinic acid (Sigma-Aldrich), Isopropanol (Merck) and Hydrazine (Merck). All these chemicals were analytical regent and used without further purification.

Preparation of graphene nanosheets (GNs)

GNs were prepared from natural graphite by a simple microwave assisted exfoliation method using an optimized wt. ratio of natural graphite and ammonium persulfate (1:1) in a 50 ml glass beaker. To this, 5 ml of 30% hydrogen peroxide was added. This reaction mixture was sonicated for 5 minutes and then placed in a domestic microwave oven (2.45 GHz, LG, India) and irradiated at 500 W for 160 s. Under the microwave irradiation, the intercalation and exfoliation of the graphite occurred rapidly with fuming and lightening without affecting the sp^2 carbon of the basal plane.[30] Once, the lightening over, then we ensured that the reaction was completed.

Preparation of Pt decorated GNs

1 wt. % of Pt decorated GNs was prepared by a simple chemical reduction method using chloroplatinic acid. Initially, an appropriate amount of GNs were dispersed in deionized water and then a required amount of chloroplatinic acid salt in isopropanol was added slowly into it with constant stirring and continued further for 12 h. To this, hydrazine was added drop by drop at pH 10 with constant stirring for 1 h. Once the reaction was completed, the mixture solution was vacuum filtered and dried at 80 °C for overnight.

Physical and Electrochemical Characterization

The crystalline structure of GNs and platinum decorated GNs were determined by X-ray diffraction studies (Rigaku, Model: Ultima IV). The confocal micro-Raman spectrometer with a laser beam of 514 nm was used to identify the fundamental properties and microstructure of carbonaceous materials (Renishaw, Model: RM 2000). The surface morphologies of the prepared GNs and 1 wt.% of Pt decorated GNs were observed by scanning electron microscope (Hitachi, Model: S-3400N).The amount of Pt decorated on the GNs was estimated by energy dispersive X-ray spectroscopy (EDX) which is equipped with SEM. The particle size and crystalline quality of the Pt decorated GNs were confirmed by transmission electron microscope and SAED studies (Philips, Model:CM200). The electrochemical impedance and cyclic voltammetry measurements were done with electrochemical workstation (VSP, Bio-Logic, France). The cyclic voltammetry study was performed in a three electrode cell to investigate the electrocatalytic properties of counter electrode towards the reduction of triiodide ion in the redox mediator. It consisted of the prepared CE material with an active area of 0.25 cm^2 as working electrodes, Pt as counter electrode with an active area of 1 cm^2 and Ag/AgCl as the reference electrode and 0.01 M LiI, 0.001 M I_2 and 0.1 M $LiClO_4$ in acetonitrile as an electrolyte in the potential range of -1.0 to 1.0 V at various scan rates. The electrochemical impedance measurements (EIS) were carried out using symmetric cells for std. Pt, GNs and Pt-GNs electrodes. The surlyn tape was used between two symmetrical electrodes as the spacer to calculate the charge transfer resistance (R_{ct}) in the frequency range of 100 KHz to 1 mHz. The Tafel polarization measurements were performed at the scan rate of 50 mV s^{-1} using the same symmetrical cells to verify the electrocatalytic activity of the CE by knowing its exchange current density.

Fabrication of DSSC

First, the ITO glass plates were cleaned subsequently with acetone, ethanol and deionized water in an ultrasonic water bath to remove organic impurities and then dried in air. The ITO glass plates are selected due to its low surface roughness and high electrical conductivity than the FTO glass plates. [32, 33] Scotch tape was employed as a spacer to control the film thickness and to provide uncoated area for electrical contact.[34] The TiO_2 paste (Dyesol Ltd) was spread over the spacer between the scotch tape and conducting glass substrate using doctor blade technique and then dried in air at 30 °C for 10 min. and sintered at 450 °C for 30 min. to remove any organic matter. The thickness of the photo anode film was ca. 12 μm thickness and its area was 0.20 cm^2. The sintered photoanode was cooled down to 80 °C and immersed in a solution containing 3×10^{-4} M of dye, Di-tetrabutyl ammonium cis-bis(isothiocyanato) bis (2,2'-bipyridyl-4,4'-dicarboxylato) Ruthenium(II) for 24 h. This dye-sensitized TiO_2 photoanode was then cleaned with anhydrous ethanol to remove excess dye and dried in moisture free air. The counter electrodes waere prepared by slurry coating procedure. The mixture containing exfoliated graphene or Pt-GNs and poly (vinylidenefluoride) in the ratio of 95:5 wt% in N-methyl-2-pyrrolidone was finely ground together using mortar. Subsequently, the paste was coated with 10 μm thickness on pretreated ITO plate using the doctor blade technique and then dried for 12 h at 80 °C in a vacuum oven.

The TiO_2 photoanode was assembled with various counter electrodes such as std. Pt paste (Dyesol Ltd.), GNs and 1 wt.% of Pt decorated GNs separately, using a hot press at 110 °C. The I^-/I_3^- redox electrolyte which consisted of 0.5 M of LiI, 0.05 M of I_2,0.5 M of TBP and 0.5 M of 1-butyl-3-methylimidazolium iodide (ionic liquid) in acetonitrile was injected into the cells

through two small holes drilled in the counter electrode. The holes were then covered and sealed with small squares of surlyn tape. [35]

Photovoltaic performance

Photovoltaic performance of the fabricated DSSCs were evaluated using a calibrated AM 1.5 solar simulator (Newport, Oriel instruments USA 150W, model: 67005) with a light intensity of 100 mW cm^{-2}, calibrated using standard mono-crystalline silicon solar cell (Newport, Oriel instruments, model: 91150V) and a computer controlled digital source meter (Keithley, Model: 2420).The light-to-electricity conversion efficiency (η) of the assembled cells were calculated from the measured photoelectro-chemical parameters such as fill factor (FF), open circuit voltage (V_{oc}), short circuit current density (J_{sc}) and incident optical power (P_{in}).

Results and discussion

The XRD patterns of the natural graphite, GNs and 1 wt.% of Pt decorated GNs are shown in Fig. 1. The characteristic high intense (002) peak appears at 2θ=26.7˚ for the natural graphite with high magnitude of nearly 4,00,000 and one more small intense peak appears at 2θ=55˚ confirms a highly organized crystalline structure of hexagonal graphite. [36] In contrast, similar peaks are found in GNs with sharp and low intense peak at 2θ= 26.6˚ and 55.1˚ indicate the formation of exfoliated graphene nanosheets. [37] The peak height with decreased magnitude of several order suggests that the exfoliated graphene nanosheets size is reduced to nanometer level. The interplanar spacing (0.332 nm) of GNs also measured from XRD pattern. X-ray diffraction pattern of 1 wt.% of Pt decorated-GNs exhibits the characteristic sharp diffraction peaks at 2θ=39.8˚ (1 1 1) and at 2θ=46.2˚ (2 0 0) which specifies the face-centered cubic (fcc) platinum

crystalline lattice and this has good agreement with the JCPDS data. [38] This confirms that the platinum precursor, H_2PtCl_6 has been reduced completely to platinum by hydrazine.

Raman spectroscopy is a useful tool to distinguish the degree of ordered and disordered carbon structures. The Raman spectra of GNs and 1 wt.% of Pt- GNs are shown in Fig. 2. The G band is usually assigned to the E_2g phonon of sp^2 C atoms which is connected to the graphitic hexagon-pinch mode and the D band raised from a breathing mode of point photons of A_1g symmetry, which corresponds to the defects in graphene sheet. Raman spectra of GNs show a G band at 1579 $cm^{-1}$and D band at 1373 $cm^{-1}$and a weak second order 2D band at 2722 cm^{-1}. [39-41] The disorder induced band (D band) is found at 1350 cm^{-1} for the prepared Pt- GNs with a very low intensity, suggesting that it is nearly defect free. The ratio between the intensity of D and G bands is generally used to predict the presence of defects and the size of the in-plane sp^2 domain. The intensity ratio of I_D/I_G (R) for Pt- GNs is found to decrease (0.89) relative to GNs (1.1). This significant decreased R value of Pt- GNs is attributed to the decrease in size of the in-plane sp^2 domains and a partially ordered crystal structure of Pt- GNs.

The microstructures of exfoliated graphene and Pt decorated GNs are shown in Fig. 3 (a & b). From Fig. 3(a), it can be seen that GNs exhibited flat, smooth and very thin layered structure but the sheets are randomly crumpled indicating that the ordered thick layered structure of natural graphite precursor has been disrupted due to microwave irradiation. [42] From Fig. 3(b), it can be seen that the presence of Pt nanoparticles on GNs and these Pt nanoparticles are evenly dispersed throughout the GNs. This may help to enhance the electrocatalytic redox behavior of I_3^-/ I^-. Fig. 3(c) shows the EDX spectrum of Pt decorated GNs. The amount of Pt decorated on the GNs was confirmed by EDX and it was found to be ~ 1.02 wt. %.

TEM images of Pt decorated GNs are shown in Fig. 4(a-c). It can be seen that the fine Pt nanoparticles in the range of 2-3 nm are well dispersed over the GNs. SAED pattern of Pt-GNs is shown in Fig. 4(a-c). The SAED pattern is indexed to the (111), (200) and (220) reflections of face-centered cubic platinum, which is consistent with the results of the XRD pattern (Fig.4d). The randomly weak and diffuse diffraction rings represents the loss of long range ordering in the GNs. In addition, the sharp diffraction spots revealed the polycrystalline structure of Pt nanoparticles.

Cyclic voltammetry analysis is an effective tool to investigate the electro-catalytic activity of the prepared counter electrode by the relation between ion (I^-/I_3^-) diffusivity and reaction kinetics using three electrode system. The higher electrocatalytic activity towards the I_3^-/ I^- redox process is an essential factor for efficient CEs. The cyclic voltammograms show oxidation and reduction kinetics of I_3^-/I^- redox couple as follows**;**

$$3I^- \rightleftharpoons I_3^- + 2e^- \quad \text{Oxidation} \qquad (1)$$

$$I_3^- + 2e^- \rightleftharpoons 3I^- \quad \text{Reduction} \qquad (2)$$

The relative positive pair (right) of anodic peak is due to the oxidation reaction and the negative pair of cathodic peak (left) is associated with the reduction reaction. The negative pair of cathodic peaks is more significant that have direct impact on the photovoltaic performance of DSSCs. The cyclic voltammograms are obtained for std. Pt, GNs and 1 wt.% of Pt decorated GNs at the scan rate of 50 mV s^{-1} in the potential range of -1 to 1 in an electrolyte solution contains 0.01 M LiI, 0.001 M I_2 and 0.1 M $LiClO_4$ in acetonitrile are shown in Fig. 5. The cyclic voltammogram of Pt decorated GNs has higher anodic and cathodic peak current densities and

larger electrochemical active surface area of the electrode is due to its larger enclosed redox reaction area of the CV curve. This suggesting an improved electrocatalytic redox behavior towards the reduction of I_3^- and oxidation of I^-. The relatively lesser oxidation to reduction peak separation and a positive side shifting in the reduction peak were observed in 1 wt.% of Pt decorated GNs than the std. Pt and GNs based CEs. This indicates a faster electron transfer kinetics, high electrocatalytic activity and reduction of overpotential for I_3^- reduction of 1 wt.% Pt- GNs based CEs. It revealed that the addition of platinum onto GNs has enhanced the electrocatalytic activity rather than GNs and std. Pt based CE materials.

The characteristics of cyclic voltammogram depend on the rate of electron transfer process and scan rate. Cyclic voltammograms are carried out for the prepared Pt-GNs CE material at various scan rates (5, 10, 25, 50, 100 & 200 mV s^{-1}) are shown in Fig. 6. The oxidation and reduction peak current density is linear relationship to the square root of the scan rate is shown in Fig. 7. When the scan rate increased, the cathodic peak gradually shifted to the negative direction and the corresponding anodic peak shifted to the positive direction (Fig.6). The peak shift indicates that the diffusion limitation of the redox reaction of I_3^-/ I^- at the Pt-GNs counter electrode. This phenomenon inferred that no specific interaction occurred between I_3^-/ I^- and the Pt-GNs CE.[43]

EIS measurements were carried out using the symmetric cell system to determine the interfacial resistance of the counter electrode material in an electrolyte solution which has major influence on the performance of DSSC. The high frequency region response is consigned to electrochemical charge transfer behavior occurring at the CE/electrolyte boundary. The Nyquist plots of symmetrical cells fabricated using std. Pt, GNs and 1 wt.% of Pt decorated GNs counter

electrode materials are compared with the corresponding equivalent circuit in Fig. 8. The EIS parameters such as solution resistance (R_s) and charge transfer resistance (R_{ct}) are calculated from the Nyquist plot are given in Table 1. It can be seen that the 1 wt.% of Pt- GNs has lower charge transfer resistance (2.65 Ω) than std. Pt (3.12 Ω). This indicates that the charge transfer processes occurred faster by utilizing the maximum surface of Pt- GNs rather than the surface of std. Pt. As a result, the higher anodic and cathodic peak current densities were obtained in the cyclic voltammogram.[44] The lower values of R_{ct} also lead to better photovoltaic performance.

The interfacial charge transfer properties of iodide/triiodide redox couple on the counter electrode are evaluated by Tafel plots. The logarithmic current density (J) as a function of voltage (V) at room temperature is shown in Fig. 9. Theoretically, Tafel plot can be divided into three zones with respect to the overpotential such as polarization zone at low overpotential (< 120 mV), Tafel zone at medium overpotential (with a sharp slope) and the higher potential region at diffusion zone. The exchange current density (J_0) and the limiting diffusion current density (J_{lim}) are important parameters to elucidate the electrocatalytic activity of the electrodes that can be calculated from the Tafel zone and diffusion zone, respectively. The J_0 can be determined from the intersection of the extrapolated intercepts of the linear region of the anodic and cathodic curves when the overpotential is zero. The 1 wt.% of Pt- GNs electrode exhibits larger value of exchange current density and J_{lim} suggesting the higher electrocatalytic activity compared to std. Pt and GNs. [26]

The charge transfer resistance (R_{ct}) may be correlated with the exchange current density (J_0), while the triiodide is reduced to iodide at the counter electrode. The exchange current density is calculated from the charge transfer resistance using equation (3);

$$J_o = \frac{RT}{nFR_{ct}} \quad (3)$$

Where, R, T, n and F represent the gas constant, temperature, numbers of electrons transferred in the reduction reaction and the Faraday constant, respectively. Here, value of n is 2 since two electrons involved in the electrochemical reduction reaction. The exchange current density calculated from charge transfer resistance data which showed higher value of J_0 for 1 wt.% of Pt decorated GNs (4.85 mA cm^{-2}).

The photovoltaic performance parameters such as V_{oc}, $J_{sc,}$ maximum voltage (V_{max}), maximum current (J_{max}) and FF of DSSC under illumination for various counter electrodes can be calculated using the following equations;

$$\eta\ (\%) = \frac{V_{\max} J_{\max}}{P_{in}} \times 100 = \frac{V_{oc} J_{sc} FF}{P_{in}} \times 100 \quad (4)$$

$$FF = \frac{V_{\max} J_{\max}}{V_{oc} J_{sc}} \quad (5)$$

The results of voltage-current density curves for the assembled cells using std Pt, GNs and 1 wt.% of Pt decorated GNs are shown in Fig. 10. Their corresponding photovoltaic parameters are compared with reported similar systems that are given in Tables 2 and 3. From these tables, it can be observed that Pt decorated GNs exhibited 11% improvement in photovoltaic cell efficiency than the std. Pt, which is higher than that of the other similar reported systems. [22-24, 26] This is due to the high electrocatalytic redox behavior and higher charge transfer rate of 1 wt.% of Pt decorated GNs. In contrast to std. Pt, GNs showed lower PCE but higher than the previously reported values. [15-17] This can be attributed to large number of defective sites

that have been created by this method which lowers the charge transfer resistance and hence enhancing the electrocatalytic activity of the prepared GNs. [31]

Conclusion

A simple and rapid microwave assisted exfoliation method followed by a simple chemical reduction method is used to prepare Pt decorated GNs CE using natural graphite flakes and chloroplatinic acid. Raman spectroscopy confirmed the improved microstructure of Pt decorated GNs compared to GNs. By decorating platinum on GNs, the electrocatalytic redox behavior of the electrode is enhanced with decreasing the charge transfer resistance of CE. Pt decorated GNs achieved 11% improvement in photovoltaic cell efficiency (η = 5.1%) which is higher than the reported other similar systems. A very small amount of Pt addition (1 wt. %) onto GNs raised the cell efficiency (5.1%). The photovoltaic performance of DSSC using 1 wt.% of Pt decorated GNs showed higher short circuit current of 10.9 mA/cm^2 with a fill factor of 0.68. Thus, the superior photovoltaic cell performance of 1 wt.% of Pt decorated GNs could be used as a low cost alternative counter electrode for DSSCs.

Acknowledgments

The authors gratefully acknowledge the CSIR (Ref. No.01(2359)/10/EMR-II), New Delhi for the financial support and CIF, Pondicherry University, India for extending their instrumentation facilities.

References

[1] B.O' Regan, M. Grätzel, *Nature* 1991, **353,**737-740.

[2] M. Grätzel, *Inorg. Chem*. 2005, **44,** 6841-6851.

[3] A. Yella, H.W. Lee, H. N. Tsao, C. Yi, A. K. Chandiran, M. K. Nazeeruddin, E. W.G. Diau, C.Y. Yeh, S. M. Zakeeruddin, M. Grätzel, *Science* 2011,**334,** 629-634.

[4] S. Mathew, A. Yella, P. Gao, R. Humphry-Baker, B.F. E. Curchod, N. Ashari-Astani, I. Tavernelli, U. Rothlisberger, Md. K. Nazeeruddin and M. Grätzel, *Nature chemistry* 2014, **6,** 242-247.

[5] R. Cruz, D. Alfredo, P. Tanaka, A. Mendes, *J. Solar Energy* 2012, **86,**716-720.

[6] M. Grätzel, *J. Photochem. Photobiol. C: Photochem. Rev.* 2003, **4,**145-153.

[7] E. Olsen, G. Hagen, S. E. Lindquist, *Solar Energy Materials & Solar Cells* 2000, **63,** 267-273.

[8] Y. Tang, X. Pan, S. Dai, C. Zhang, H. Tian, *Key Engineering Materials* 2011, **451,** 63-78.

[9] T. N. Murakami, S. Ito, Q. Wang, M. K. Nazeeruddin, T. Bessho, I. Cesar, P. Liska, R. Humphry-Baker, P. Comte, P. P´echy, M. Grätzel, *J. Electrochem. Soc.* 2006,**153,**2255-2261.

[10] Z. Huang, X. Liu, K. Li, D. Li, Y. Luo, H. Li, W. Song, L. Q. Chen, Q. Meng, *Electrochem. Commun.* (2007),**9,** 596-598.

[11] B. Ahmmad, Y. Kusumoto, M. Abdulla-Al-Mamun, A. Mihata, H. Yang, *J. Sci. Res.* 2009,**1,**430-437.

[12] D. W. Zhang, X. D. Li, S. Chen, F. Tao, Z. Sun, X. J. Yin, S. M. Huang, *J. Solid State Electrochem.* 2009, **14,** 1541-1546.

[13] K. Suzuki, M. Yamaguchi, M. Kumagai, S. Yanagida, *Chem. Lett.* 2003,**32,**28-29.

[14] K. S. Novoselov, A. K. Geim, S. V. Morozov, D. Jiang, Y. Zhang, S. V. Dubonos, I. V. Grigorieva, and A. Firsov, *Science* 2004,**306,**666-669.

[15] T. Hsieh, B. H. Yang and J. Y. Lin, *Carbon* 2011,**49,** 3092-3097.

[16] H. Choi, S. Hwang, H. Bae, S. Kim, H. Kim and M. Jeon, *Electron. Lett.* 2011, **47,** 281-283.

[17] R. Bajpai, S. Roy, N. Kulshrestha, J. Rafiee, N. Koratkarb and D.S. Misra, *Nanoscale* 2012, **4,** 926-930.

[18] Y. Y. Dou, G. R. Li, J. Song, X.P. Gao. *Phys. Chem. Chem. Phys.* 2012, **14,** 1339-1342.

[19] G. Yue, J.Y Lin, S.Y. Tai, Y. Xiao, J. Wu, *Electrochim. Acta* 2012, **85,**162-168.

[20] Y. G. Kim, Z. A. Akbar, D. Y. Kim, S. M. Jo, and S. Y. Jang, *ACS Appl. Mater. Interfaces* 2013, **5,** 2053-2061.

[21] C.E. Cheng, C.Y. Lin, C.H. Shan, S.Y. Tsai, K. W. Lin, C.S. Chang, and F. S.S. Chien, *J. Applied Physics* 2013,**114 ,**014503-014503-5.

[22] V. D. Dao, N. T. Q. Hoa, L. L. Larina, J.K. Lee and H. S. Choi, *Nanoscale* 2013, **5 ,**12237-12244.

[23] V. Tjoa, J. Chua, S. S. Pramana, J. Wei, S. G. Mhaisalkar, and N. Mathews, *ACS Appl. Mater. Interfaces* 2012, **4 ,** 3447-3452.

[24] G.H. Guai, Q.L. Song, C.X. Guo, Z.S. Lu, T. Chen, C.M. Ng, C. M. Li, *J. Solar Energy* 2012, **86,** 2041-2048.

[25] C. Y. Liu, K. C. Huang, C. H. Wang, K. C. Ho, *Electrochimica Acta* 2012,**59,** 128-134.

[26] M.H. Yeh, L.Y. Lin , J.S. Su, Y.A. Leu, R. Vittal, C.L. Sun and K. C. Ho, *Chemelectrochem* 2014, **1 ,**416-425.

[27] H. C. Schniepp, J. L. Li, M. J. McAllister, H. Sai, M. Herrera- Alonso,D. H. Adamson, R. K. Prud'homme, R. Car, D. A. Saville, and I. A. Aksay, *J. Phys. Chem. B* 2006,**110,** 8355-8359.

[28] A. Kaniyoor, S. Ramaprabhu, *J. App. Phys.* 2011, **109,** 124308-124308-6.

[29] T. Wei, Z. Fan, G. Luo, C. Zheng, D. Xie, *Carbon* 2008, **47 ,**313-347.

[30] V. Sridhar, J.H .Jeon, I-Kwon Oh, *Carbon* 2010, **48,** 2953-2957.

[31] V. Sridhar, Jung-Hwan Jung, I-Kwon Oh, *Carbon* 2011, **49,** 4449-4457.

[32] H. Bisht, H.T. Eun, A. Mehrtens, M.A. Aegerter, *Thin Solid Films* 1999, **351,** 109-114.

[33] C.X. Guo, G.H. Guai, C.M. Li, *Advanced. Energy Materials* 2011, **1,** 448-452.

[34] Harikisun, R., Desilvestro, H., 2011. Sol. Energy 85, 1179–1188.A.R. Sathiyapriya, A. Subramania, J. Young-Sam, K. Kang-Jin, *Langmuir* 2008, **24,** 9816-9819.

[35] A.Subramania, E.Vijayakumar, N.Sivasankar, A.R.Sathiyapriya, K.Kang-Jin, *Ionics* 2013, **19,** 1649-1653.

[36] G. Wang, J. Yang, J. Park, X. Gou, B. Wang, H. Liu, J. Yao, *J. Phys. Chem. C* 2008, **112 ,**8192-8195.

[37] N. Liu, F. Luo, H. Wu, Y. Liu, C. Zhang, J. Chen, *J.Adv. Funct. Mater.* 2008, **18,** 1518-1525.

[38] M. Carmo, V.A. Paganin, J. M. Rosolen, E. R. Gonzalez, *J. Power Sources* 2005, **142,** 169-176.

[39] S. Reich, C. Thomsen, Phil. Trans. *R. Soc. Lond. A* 2004, **362,** 2271-2288.

[40] S. Guo, S. Dong, E. Wang, *ACS Nano* 2010, **4,**547-555.

[41] Y.X. Xu, H. Bai, G.W. Lu, C. Li, G.Q. Shi, *J. Am. Chem. Soc*. 2008, **130,** 5856-5857.

[42] X. Zhao, Q. Zhang, D. Chen, *Macromolecules* 2010, **43,** 2357-2363.

[43] B. He, Q. Tang, J. Luo, Q. Li, X. Chen, H. Cai, *J. Power Sources* 256 (2014) 170-177.

[44] L.H. Chang, C.K. Hsieh, M.C. Hsiao, J.C. Chiang, P.I. Liu, K.K. Ho, C.C. M. Ma, M. Y. Yen, M.C. Tsai, C.H. Tsai, *J. Power Sources* 2013,**222 ,**518-525.

Table 1 The EIS parameters for various counter electrodes

Electrodes	R_s (Ω)	R_{ct} (Ω)	J_0 (mA cm^{-2})
Pt (Standard)	5.07	3.12	4.12
GNs	6.60	6.98	1.84
Pt- GNs	7.20	2.65	4.85

Table 2 Comparison of photovoltaic performances of DSSCs based on Graphene- Pt obtained using different methods as counter electrodes.

Counter electrode	Method of synthesis	V_{oc} (V)	J_{sc} (mA cm^{-2})	FF	Cell Efficiency η (%)		% of Improvement in PCE	Ref.
					Std. Pt	Pt-Graphene		
Graphene-Pt	Modified Hummers method/Dry plasma reduction	0.71	16.66	0.66	8.18	8.56	5.0	[22]
Graphene-Pt	Modified Hummers method/ Facile Photochemical synthesis	0.72	14.10	66.9	6.29	6.77	8.0	[23]
Graphene- Pt	Electrochemical deposition	0.73	15.84	0.65	7.03	7.57	8.0	[24]
Graphene/Pt	Staudenmier method/Polyol reduction	0.69	17.77	0.70	8.58	8.79	2.5	[25]
Pt -GNs	Microwave assisted synthesis/Chemical reduction	0.69	10.90	0.68	4.60	5.10	11.0	This work

Table 3 Comparison of photovoltaic performances of DSSCs based on graphene obtained using different methods as counter electrodes

Counter electrode	Method of synthesis	V_{oc} (V)	J_{sc} (mA cm^{-2})	FF	Efficiency %	Ref.
Graphene	Modified Hummers method	0.64	6.12	0.56	2.19	[15]
Graphene	Electrophoretic deposition	0.70	5.60	0.60	2.30	[16]
Graphene	Thermal exfoliation	0.62	3.94	0.42	1.01	[17]
Graphene	Electrochemical deposition	0.56	14.32	0.26	2.03	[24]
GNs	Microwave assisted synthesis	0.73	6.90	0.64	3.20	This work

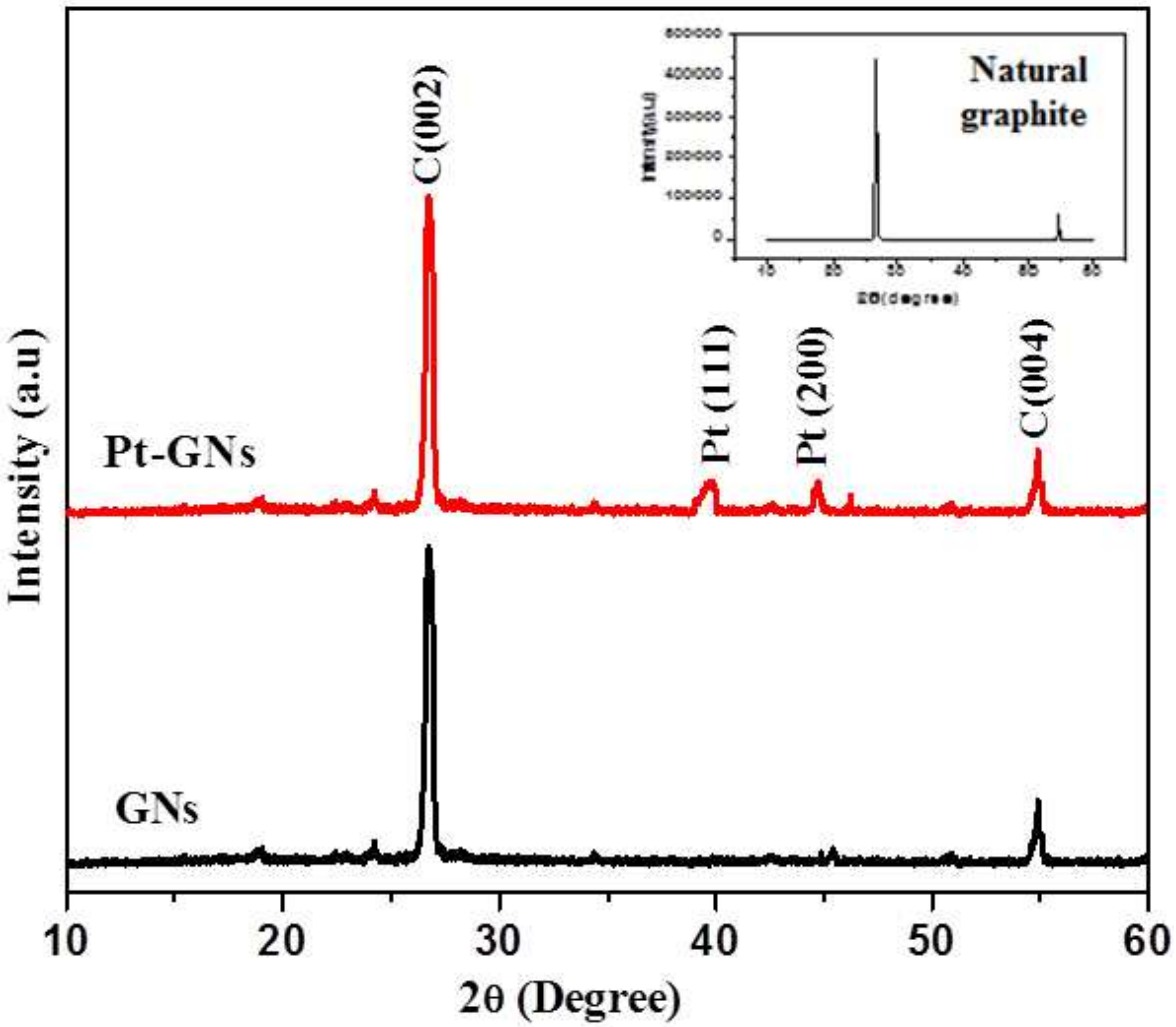

Fig. 1 XRD patterns of natural graphite, GNs and Pt decorated GNs.

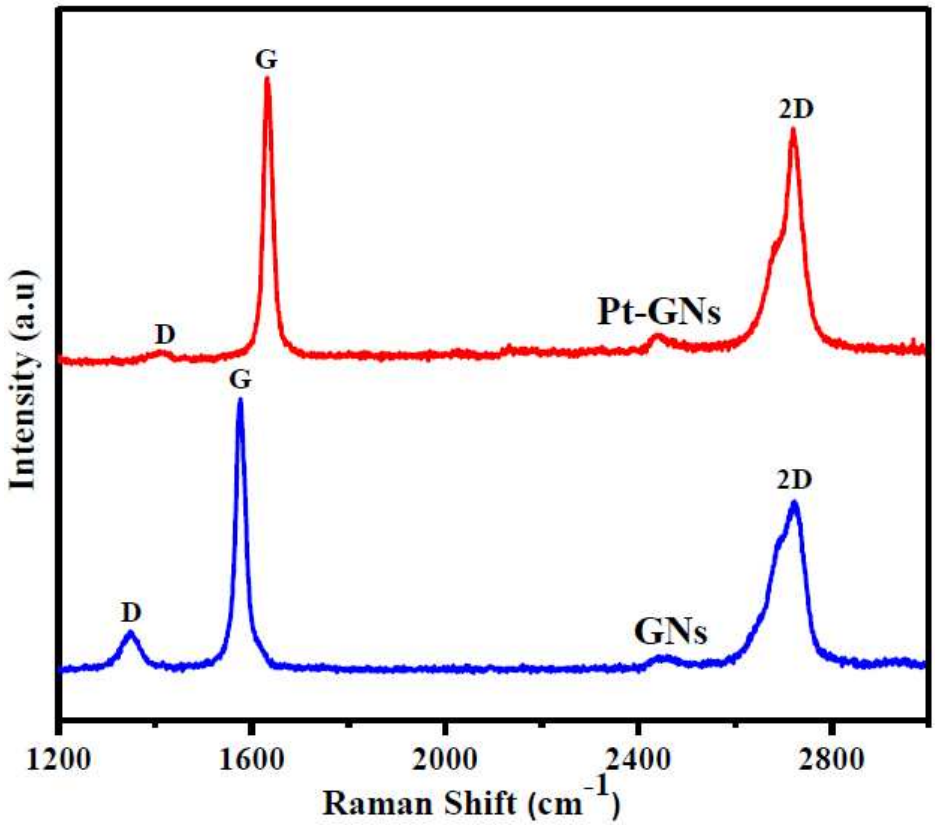

Fig. 2 Raman spectra of GNs and Pt decorated GNs.

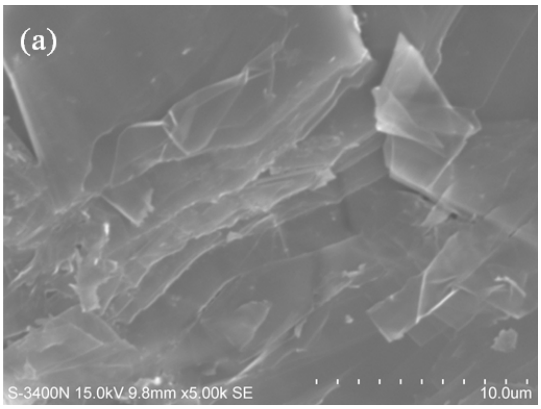

Fig. 3 SEM image of (a) GNs

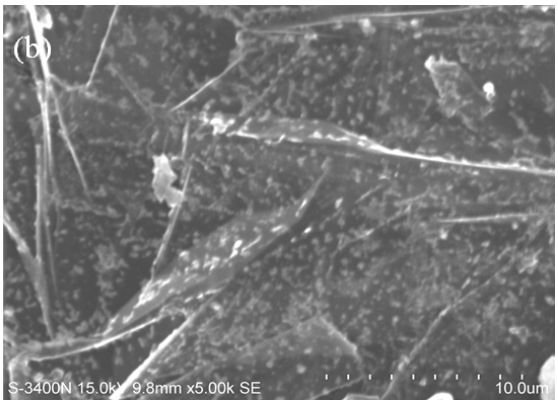

Fig. 3 SEM image of (b) Pt decorated GNs

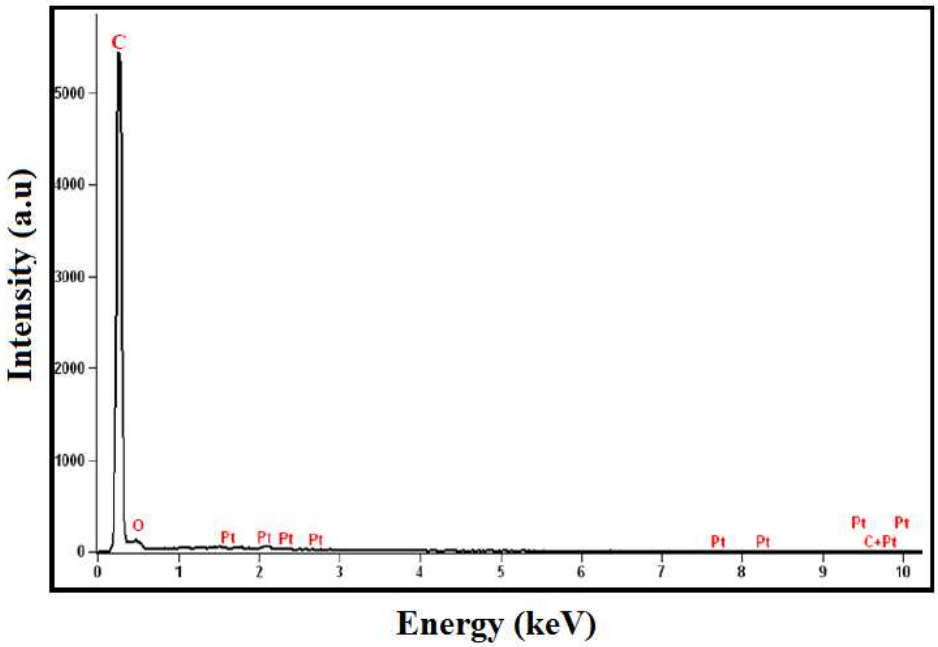

Fig. 3 (c) The EDX spectrum of Pt decorated GNs .

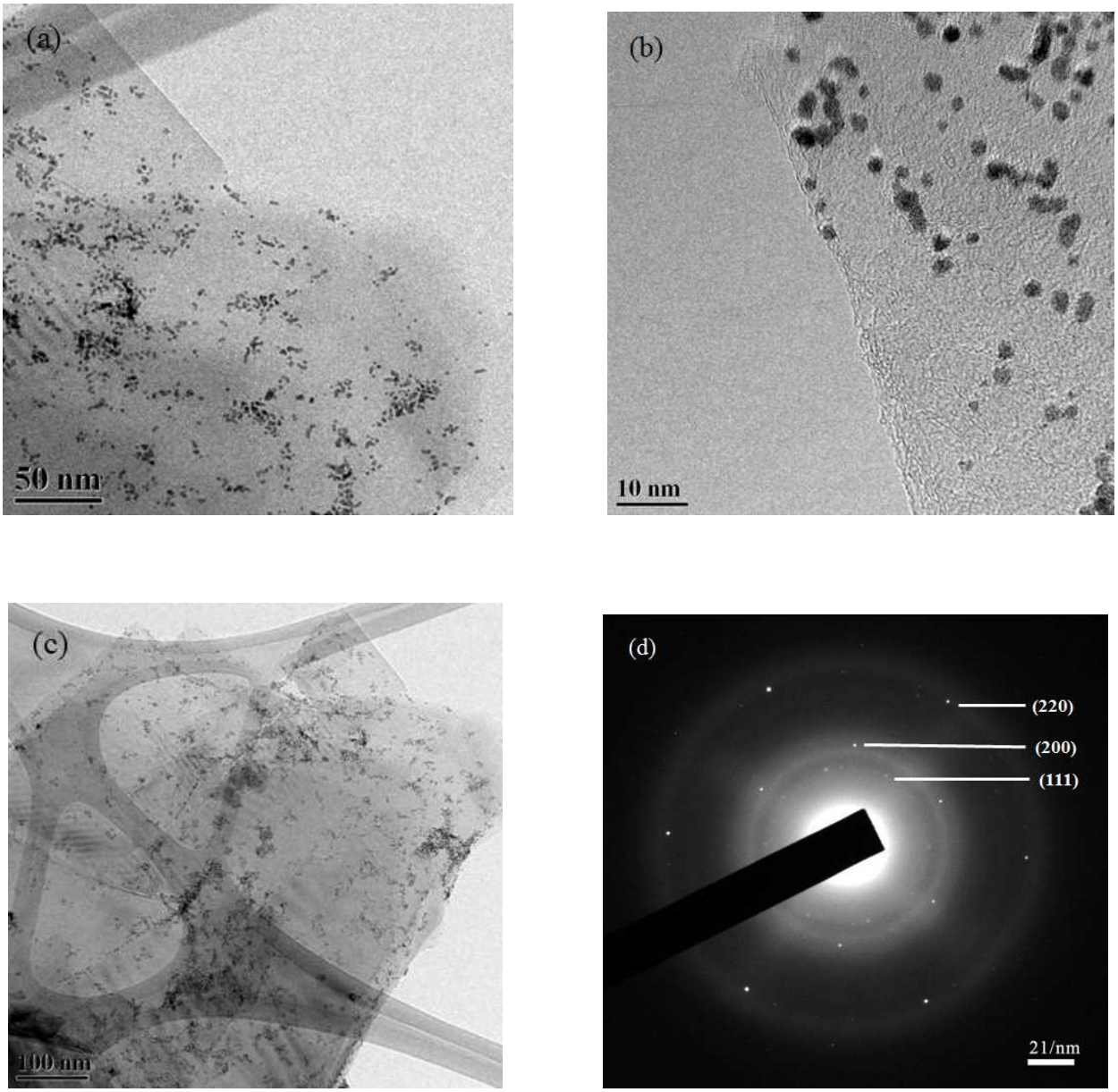

Fig. 4 (a-c) TEM images of Pt decorated GNs at different magnifications, (d) SAED pattern of Pt decorated GNs.

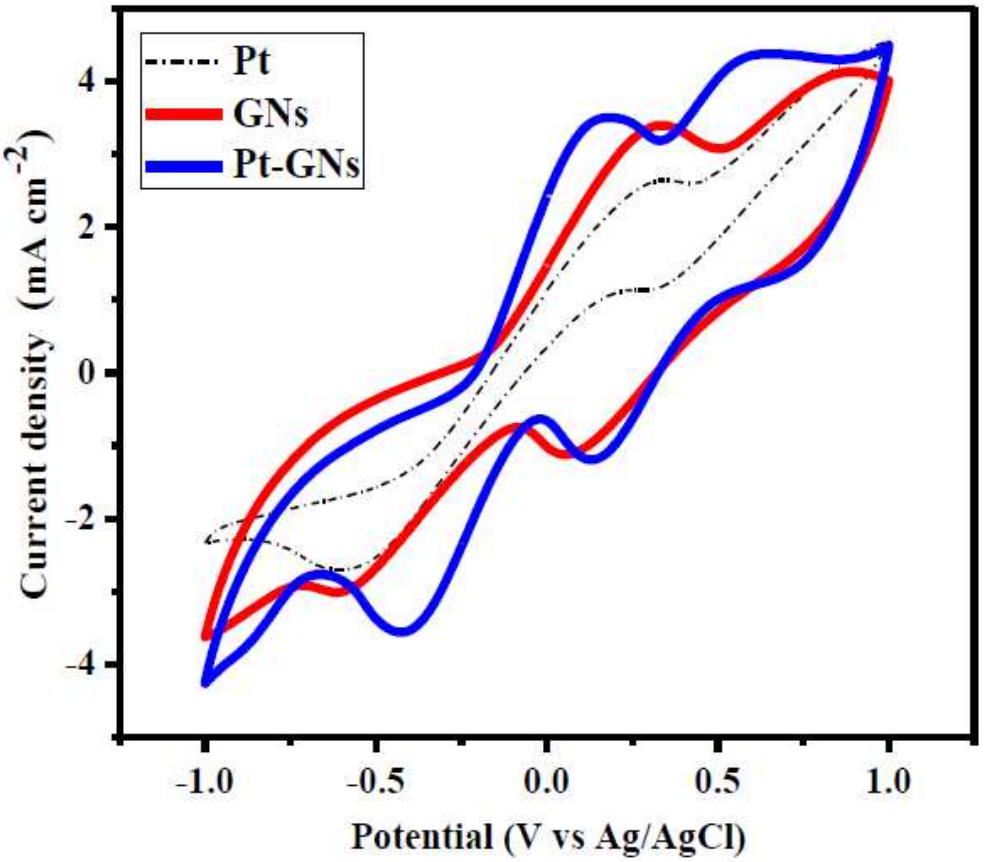

Fig. 5 Cyclic voltammograms of std. Pt, GNs and Pt decorated GNs at a scan rate of 50 mV s^{-1} in 0.01 M LiI, 0.001 M I_2 and 0.1 M $LiClO_4$ as the supporting electrolyte.

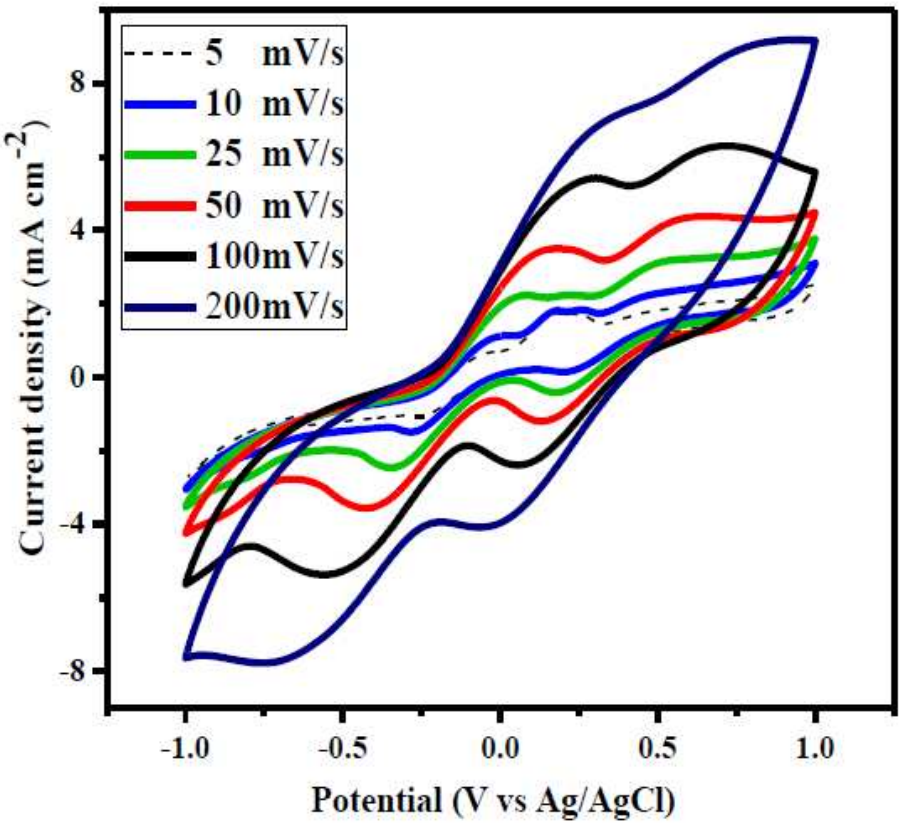

Fig. 6 Cyclic voltammograms of Pt decorated GNs as a function of different scan rates.

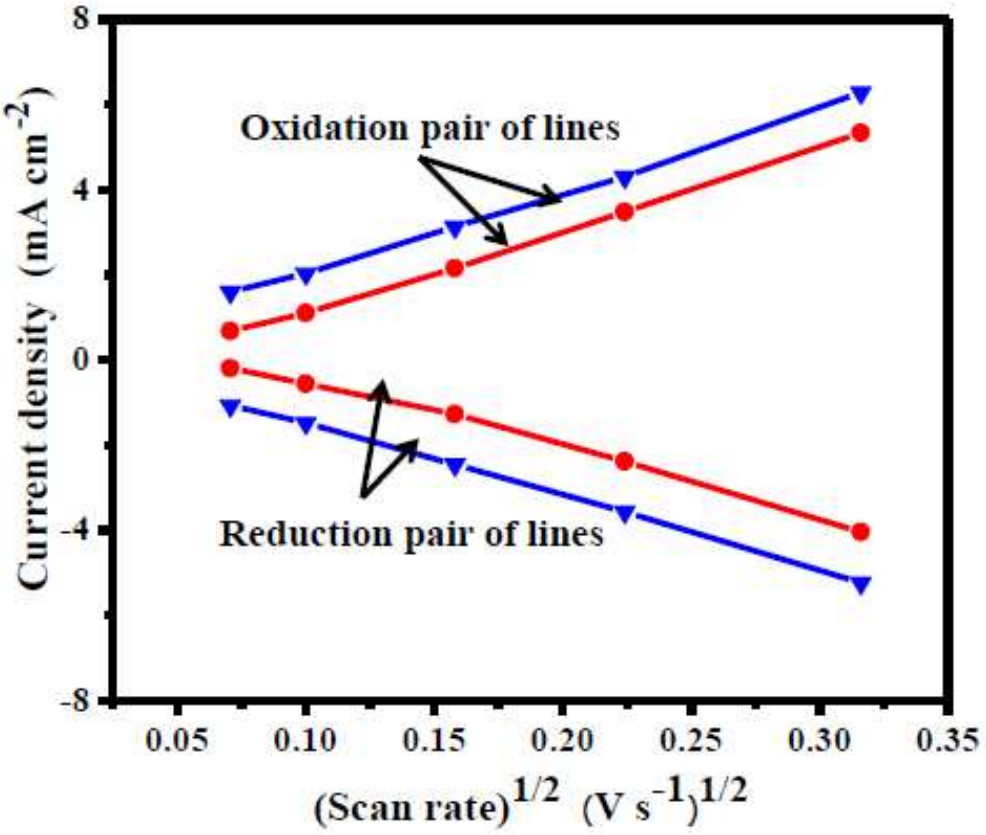

Fig. 7 The reduction and oxidation current densities of Pt- GNs electrode versus square root of different scan rates.

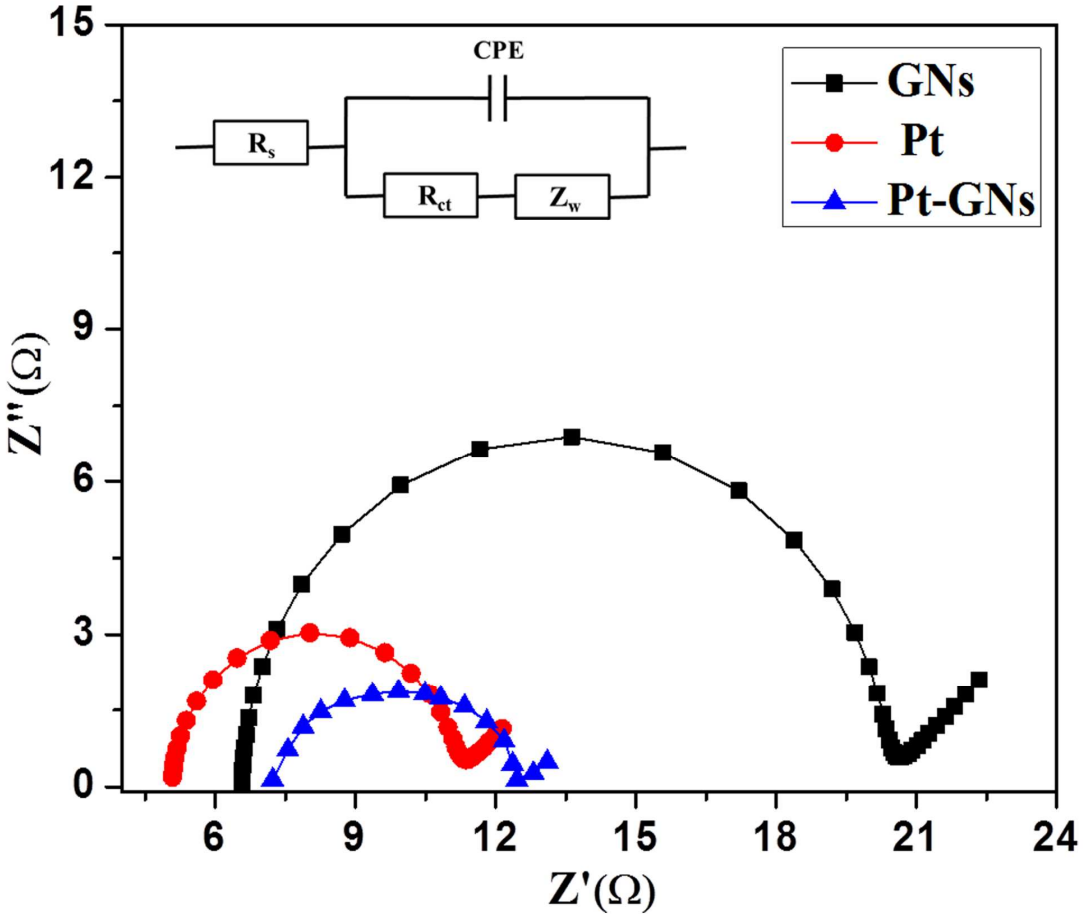

Fig. 8 Nyquist plots of std. Pt, GNs and Pt decorated GNs obtained using symmetrical cell.

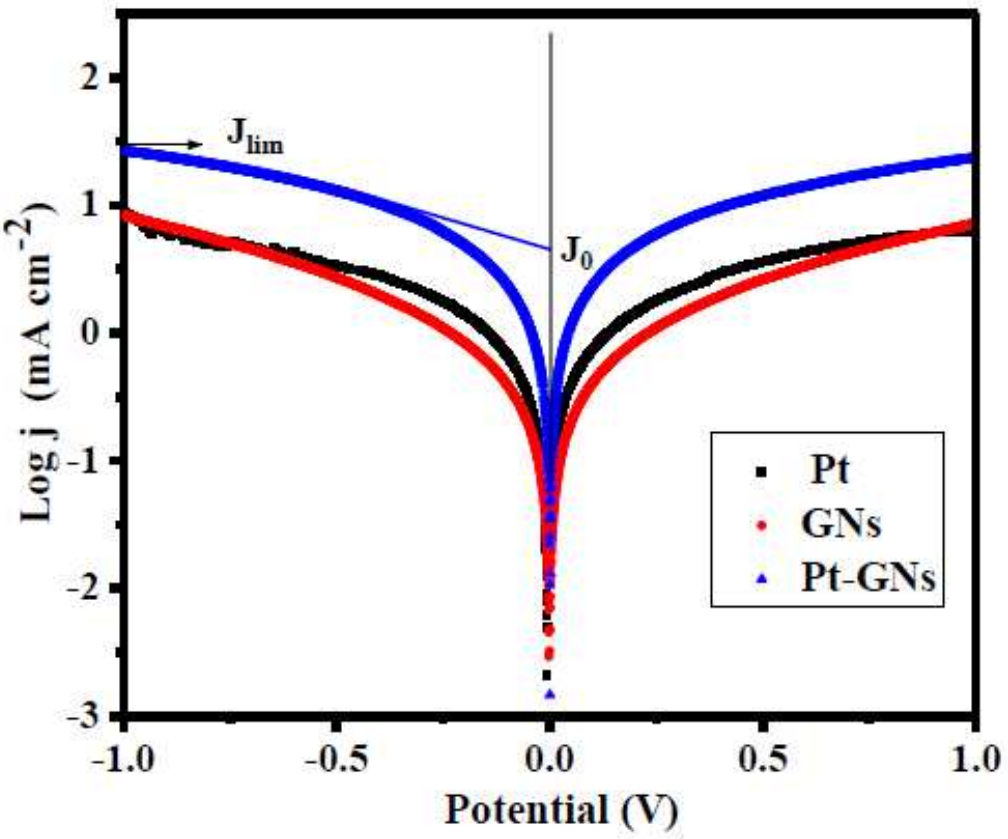

Fig. **9** Tafel curves of the symmetrical cells fabricated with two identical std. Pt, GNs and Pt- GNs electrodes.

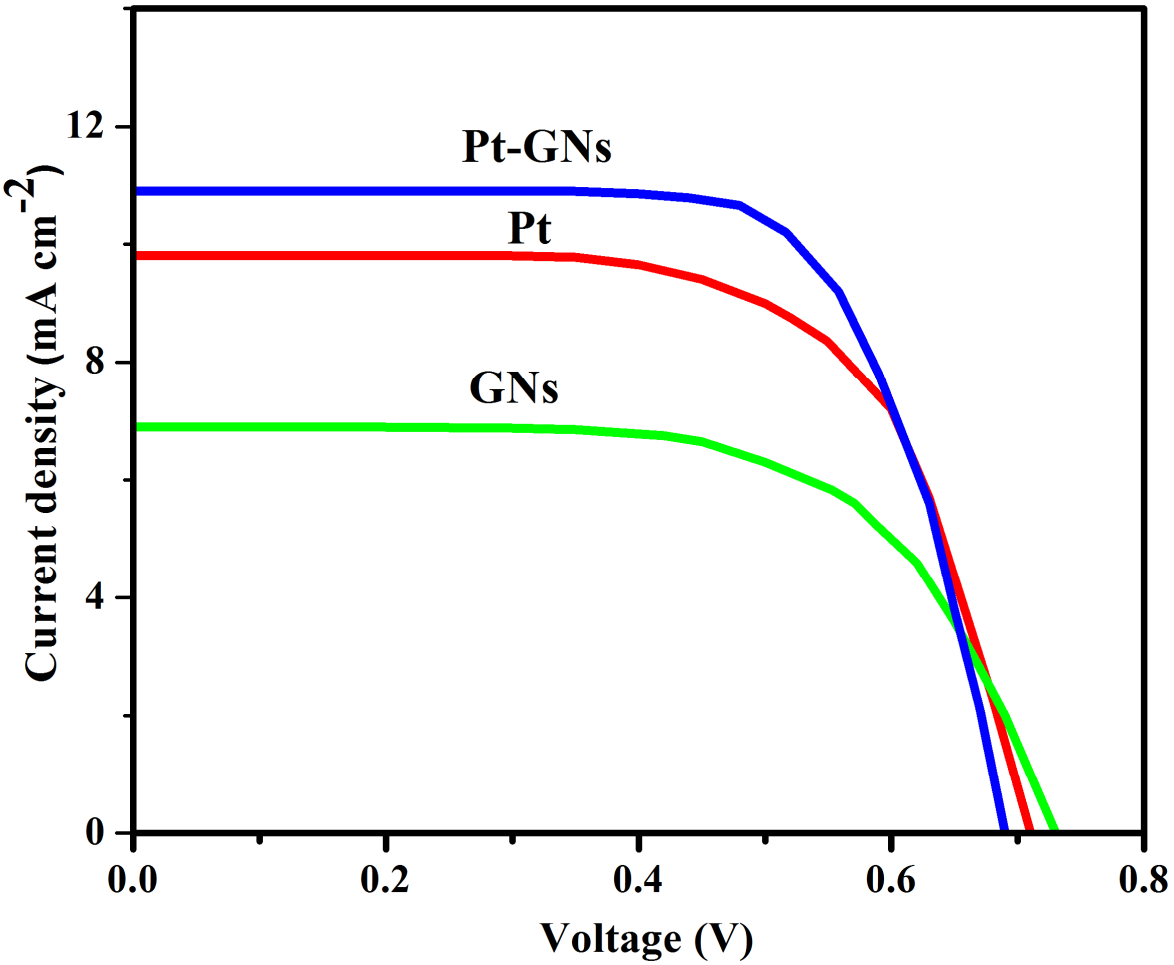

Fig. 10 I-V characteristics of DSSCs based on various std. Pt, GNs and Pt decorated GNs counter electrodes.

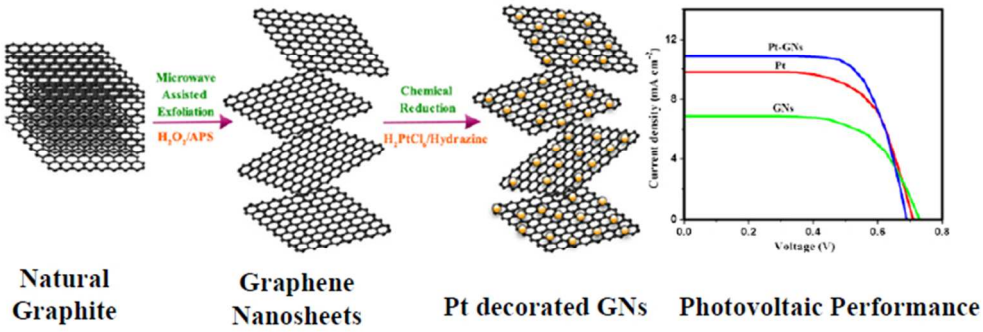

66x25mm (300 x 300 DPI)